Exciton Green's-function approach to optical absorption in a quantum well with an applied electric field

Shun-Lien Chuang
Department of Electrical and Computer Engineering, University of Illinois at Urbana-Champaign, 1406 West Green Street, Urbana, Illinois 61801

Stefan Schmitt-Rink
AT&T Bell Laboratories, Murray Hill, New Jersey 07974-2070

David A. B. Miller and Daniel S. Chemla
AT&T Bell Laboratories, Holmdel, New Jersey 07733-1988

(Received 19 June 1990)

An exciton Green's function is derived and used to calculate the polarization-dependent optical absorption in a semiconductor quantum well with an applied electric field. With use of the exciton (or Coulomb) Green's-function approach, the optical-absorption coefficient due to the bound and continuum states of excitons can be obtained simultaneously and this approach also takes into account the coupling between different subband pairs. This is in contrast with the conventional approach in which the 1*s* exciton bound state is calculated variationally and the continuum states are calculated simply using the Sommerfeld enhancement factor from the pure two-dimensional case without the correct quantum size effect. Also, the coupling between different subband pairs is usually neglected. We compare the numerical results of the Green's-function method with those of the commonly used variational method and find that the variational method overestimates the oscillator strength by 20% for the 1*s* bound state and by 50% for the continuum, although the 1*s* bound-state energy can be quite accurate. The numerical results using the exciton Green's function are compared with experimental data and found to be in very good agreement.

I. INTRODUCTION

Quantum-well optoelectronics has become a very interesting and dynamic field of research because of its potential applications in devices including improved lasers, and novel high-performance electro-optical modulators and photodetectors. Interesting fundamental quantum-mechanical phenomena can be controlled experimentally by tailoring the band structure of the semiconductor heterojunction profiles. Since the earlier research on quantum confined Stark effects,[1,2] a tremendous amount of effort has been expended to investigate both the theoretical and experimental aspects of the linear and nonlinear optical properties of semiconductor quantum wells and the exciton effects. For a review of the linear properties including the electric-field effects and the nonlinear properties, see Ref. 3.

The theoretical calculations for the linear absorption coefficient are either (1) using variational method[1,4] for the bound 1*s* exciton state and the pure two-dimensional Coulomb enhancement factor[5] for the continuum states within the parabolic model, or (2) taking into account the valence-band-mixing effects and solving the bound-exciton problem variationally[6] or numerically[7,8] with approximations for the Coulomb potential. Until recently, a direct numerical approach was used to solve for the exciton wave functions in quantum wells and to calculate the absorption coefficient.[9–11] However, a large number of basis functions have to be used[9] because of the singular nature of the Coulomb potential in momentum space.

In this paper, we present an alternative approach based on the exciton Green's function to calculate the absorption coefficient. It is also called the Coulomb Green's function and was introduced[12] in the coordinate space for applications involving perturbations of the ground state of the hydrogen atom and later was applied to the exciton problem.[13,14] Its momentum-space representation has also been very useful recently in the study of the optical Stark effect.[14–17] The Green's function satisfies an inhomogeneous Coulomb wave equation for an electron-hole pair with the dipole moment as the source term. The equation is similar to the exciton (hydrogen) wave equation and contains terms such as the single-particle electron and hole Hamiltonians with the Coulomb interaction except that the total energy is shifted by the photon energy, and the driving source term is the optical dipole moment.

Previously, the exciton Green's function was used in the study of the exciton polarizations[13] and optical Stark effect. It was solved in the purely two- and three-dimensional limits.[14] However, because of the numerical nature of the approach, very little work has been done in applying it to the problem of the real, finite-size, quantum wells. In this paper, we show numerical results calculated using this technique for the linear absorption coefficient in finite wells with applied electric fields, properly taking into account the singularities of the Coulomb potential in the momentum space. We compare the nu-

merical results of the exciton Green's-function method with those using the variational method.[1,4] We find that although the variational method may give very accurate results for the binding energy of the lowest bound exciton in the quantum well, its numerical values for the oscillator strength may differ by 20%. This agrees with the essence of the variational concept since a first-order error in the trial wave function usually results in second-order errors in the energy when the binding energy is minimized. The oscillator strength is simply determined by the square of the wave function at $\rho=0$, where ρ is the separation between the electron and hole in the plane of the well interface. For absorption above the band edge, in previous work usually the pure two-dimensional (2D) Coulomb enhancement factor for the continuum states is used. We show that the pure 2D enhancement factor overestimates the absorption coefficient by a factor of about 1.5 for a (100 Å GaAs)/$Al_{0.3}Ga_{0.7}As$ quantum well.

In Sec. II, we derive the relation between the absorption coefficient and the exciton Green's function for a quantum well with a general profile. We then show the solution technique for the Green's function taking into account the singular nature of the Coulomb potential in Sec. III. For convenience in calculations and physical interpretations, normalized dimensionless quantities with an undertilde symbol are used, unless specified otherwise. For example, the exciton energy E_x is normalized by the exciton rydberg R_0, $\underset{\sim}{E}_x=E_x/R_0$. The comparison with the variational method is discussed in Sec. IV with both analytical and numerical results. In Sec. V, we compare our results with the experimental data for the polarization-dependent absorption coefficient. The conclusions are given in Sec. VI. Only the linear susceptibility is considered in this paper. Further applications of the exciton Green's function to optical nonlinear susceptibility[18,19] are in progress.

II. OPTICAL SUSCEPTIBILITY AND THE EXCITON GREEN'S FUNCTION

In this section, we use the density matrix approach to derive the optical susceptibility for a quantum well with an applied electric field. The final expression for the optical susceptibility is expressed in terms of the exciton Green's function.

Following the density-matrix approach as in Shen,[20] the linear susceptibility can be written in SI units in the following form:

$$\epsilon_0\chi_{ij}(\omega)=\frac{2}{V}\sum_{a,b}\frac{M_{ab}^i M_{ba}^j}{E_b-E_a-\hbar\omega-i\Gamma}\ , \tag{1}$$

where the factor of 2 accounts for the spins, M_{ab}^i is the ith spatial component of the dipole matrix element M_{ab} (i.e., $i=x,y,z$), which is defined as

$$\mathbf{M}_{ab}=\langle a|e\mathbf{R}|b\rangle \tag{2}$$

and[21,22]

$$\mathbf{R}=\sum_{l=1}^{N}\mathbf{r}_l\ , \tag{3}$$

i.e., summing over all the electrons in the crystal. The initial state a is taken to be the ground state $|g\rangle$, i.e., the valence band being fully occupied and the conduction band empty. The final state b is assumed to be the exciton state $|X\rangle$, which can be either a bound state of the exciton or an excited scattering state of an electron and a hole in the continuum. The energy difference E_b-E_a is E_X, which is the exciton energy measured from the ground state. The linear optical susceptibility can be rewritten as

$$\epsilon_0\chi_{ij}(\omega)=\frac{2}{V}\sum_{X}\frac{M_{gX}^i M_{Xg}^j}{E_X-\hbar\omega-i\Gamma}\ . \tag{4}$$

The free electron and hole state without Coulomb interaction can be defined[8,21,22] in the following manner. $|nm\mathbf{k}\rangle$ is the state obtained by replacing a single electron in the valence band $|m\mathbf{k}\rangle$ by an electron in the conduction band $|n\mathbf{k}\rangle$, where $\mathbf{k}$ is the wave vector in the x-y plane, and n and m are the electron and hole subband indices, respectively (Fig. 1). The exciton state $|X\rangle$ can be expanded as a linear combination of the above states[8]

$$|X\rangle=\sum_{n,m,\mathbf{k}}\phi_{nm}^X(\mathbf{k})|nm\mathbf{k}\rangle\ . \tag{5}$$

The matrix element can be reduced from an N-particle operator form to a single-particle operator form[21,22]

$$\begin{aligned}\langle nm\mathbf{k}|e\mathbf{R}|g\rangle&=\langle\Psi_{n\mathbf{k}}^c|e\mathbf{r}|\Psi_{m\mathbf{k}}^h\rangle\\&=\mu_{nm}(\mathbf{k})\ ,\end{aligned} \tag{6}$$

and the result[23–26] is discussed in Appendix A. The single electron state $\Psi_{n\mathbf{k}}^c$ and the single-hole state $\Psi_{m\mathbf{k}}^h$ satisfy

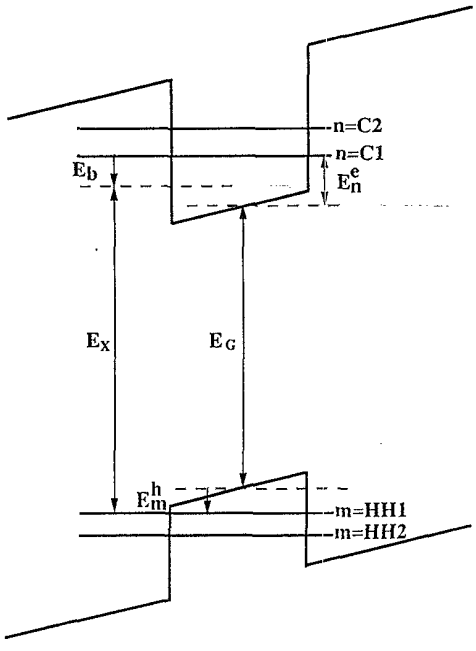

FIG. 1. A quantum well in the presence of an applied electric field.

$$\left[-\frac{\hbar^2}{2m_e^*}\nabla^2+V_e(z)+|e|Fz\right]\Psi^c_{n\mathbf{k}}(\mathbf{r})=E^e_n(\mathbf{k})\Psi^c_{n\mathbf{k}}(\mathbf{r}) , \quad (7a)$$

$$\left[-\frac{\hbar^2}{2m_h^*}\nabla^2+V_h(z)-|e|Fz\right]\Psi^h_{m\mathbf{k}}(\mathbf{r})=E^h_m(\mathbf{k})\Psi^h_{m\mathbf{k}}(\mathbf{r}) , \quad (7b)$$

respectively, where m_e^* and m_h^* are the effective masses, $V_e(z)$ and $V_h(z)$ are the quantum-well potentials for the electrons and holes, respectively, $|e|$ is the charge of a hole, and F is the electric field. The electron and hole wave functions can be written as

$$\Psi^c_{nk}(\mathbf{r})=f_n(z)\frac{e^{i\mathbf{k}\cdot\rho}}{\sqrt{A}}u_c(\mathbf{r}) , \quad (8a)$$

$$\Psi^h_{mk}(\mathbf{r})=g_m(z)\frac{e^{i\mathbf{k}\cdot\rho}}{\sqrt{A}}u_v(\mathbf{r}) , \quad (8b)$$

where A is the area in the plane of the interface, and $u_c(\mathbf{r})$ and $u_v(\mathbf{r})$ are the periodic parts of the Bloch functions, assumed to be the same for the well and barrier materials. The optical matrix element becomes

$$\langle X|e\mathbf{R}|g\rangle=\sum_{n,m,\mathbf{k}}\phi^{X*}_{nm}(\mathbf{k})\mu_{nm}(\mathbf{k}) . \quad (9)$$

The amplitude $\phi^X_{nm}(\mathbf{k})$ satisfies the effective-mass equation for excitons in a quantum well[8]

$$E_{nm}(k)\phi^X_{nm}(\mathbf{k})-\sum_{n',m',\mathbf{k}'}\langle nm|V_{\mathbf{k}-\mathbf{k}'}|n'm'\rangle\phi^X_{n'm'}(\mathbf{k}')=E_X\phi^X_{nm}(\mathbf{k}) , \quad (10)$$

where

$$E_{nm}(k)=E_G+E^e_n(k)+E^h_m(k) \quad (11)$$

and

$$E^e_n(k)=E^e_n+\frac{\hbar^2k^2}{2m_e^*}, \quad E^h_m(k)=E^h_m+\frac{\hbar^2k^2}{2m_h^*} .$$

The Coulomb potential with the quantum-well size effect is

$$\langle nm|V_{\mathbf{k}-\mathbf{k}'}|n'm'\rangle=\frac{e^2}{2\epsilon|\mathbf{k}-\mathbf{k}'|A}\int dz_e\int dz_h\, f^*_n(z_e)g^*_m(z_h)e^{-|\mathbf{k}-\mathbf{k}'||z_e-z_h|}f_{n'}(z_e)g_{m'}(z_h) . \quad (12)$$

The exciton Green's function is expressed as[14,15]

$$G^j_{nm}(\mathbf{k},\hbar\omega+i\Gamma)=\sum_X\phi^X_{nm}(\mathbf{k})\left[\frac{\sum_{n',m',\mathbf{k}'}\phi^{X*}_{n'm'}(\mathbf{k}')\mu^j_{n'm'}(\mathbf{k}')}{E_X-\hbar\omega-i\Gamma}\right] , \quad (13)$$

where $\hbar\omega$ is the photon energy, Γ is the half-linewidth due to dephasing, and superscript j refers to the jth spatial component of the dipole moment. The optical susceptibility can be written in terms of the exciton Green's function in the following form:

$$\epsilon_0\chi_{ij}(\omega)=\frac{2}{V}\sum_{n,m,\mathbf{k}}\mu^{i*}_{nm}(\mathbf{k})G^j_{nm}(\mathbf{k},\hbar\omega+i\Gamma) . \quad (14)$$

The exciton Green's function satisfies the following integral equation in momentum space, similar to Eq. (10) for the envelope function of the exciton:

$$[E_{nm}(k)-\Omega]G^j_{nm}(\mathbf{k},\Omega)-\sum_{n',m',\mathbf{k}'}\langle nm|V_{\mathbf{k}-\mathbf{k}'}|n'm'\rangle G^j_{n'm'}(\mathbf{k}',\Omega)=\mu^j_{nm}(\mathbf{k}) , \quad (15)$$

where $\Omega=\hbar\omega+i\Gamma$. A comparison of Eqs. (15) and (10) shows that the eigenvalues E_X and the eigenfunctions have to be solved in (10), while the integral equation with the dipole moment as the source term has to be solved for the exciton Green's function (15). To show that the exciton Green's function indeed satisfies (15), we expand the Green's function in terms of the exciton envelope functions assuming that they form a complete set:

$$G^j_{nm}(\mathbf{k},\Omega)=\sum_X\phi^X_{nm}(\mathbf{k})c^j_X , \quad (16)$$

where

$$\sum_{n,m,\mathbf{k}}\phi^{X*}_{nm}(\mathbf{k})\phi^{X'}_{nm}(\mathbf{k})=\delta_{XX'} . \quad (17)$$

Substituting (16) into (15) and making use of (10), then multiplying by the complex conjugate of the envelope function ϕ^{X*}_{nm} and summing over n, m, and $\mathbf{k}$, we find that c^j_X is given by the expression in the large parentheses in (13). Thus, we prove (15). Let us consider either $i=j=x$ (or y for TE polarization) or $i=j=z$ (for TM polarization) and drop superscripts i and j without loss of clarity. The absorption coefficient is calculated from the imaginary part of the optical susceptibility:

$$\alpha=\omega\epsilon_2/(n_Rc\epsilon_0) , \quad (18a)$$

$$\epsilon_2=\mathrm{Im}[\epsilon_0\chi(\omega)] . \quad (18b)$$

III. SOLUTION FOR THE EXCITON GREEN'S FUNCTION

To solve the exciton Green's function satisfying

$$[E_{nm}(k)-\Omega]G_{nm}(\mathbf{k},\Omega)-\sum_{n',m',\mathbf{k}'}\langle nm|V(\mathbf{k}-\mathbf{k}')|n'm'\rangle G_{n'm'}(\mathbf{k}',\Omega)=\mu_{nm}(\mathbf{k}) \quad (19)$$

the singularity of the Coulomb potential must be taken into account properly. Here we assume that G depends on the magnitude of $\mathbf{k}$ only, since only the s states of the exciton wave functions contribute to the linear absorption. We first subtract the singular part of the potential and write

$$\langle nm|V(q)|n'm'\rangle=\frac{1}{A}\langle nm|V^{(1)}_{\mathbf{k},\mathbf{k}'}|n'm'\rangle + \frac{1}{A}V^{(2)}(q)\delta_{nn'}\delta_{mm'} , \tag{20}$$

where

$$\mathbf{q}=\mathbf{k}-\mathbf{k}' , \tag{21}$$

$$q=[k^2+(k')^2-2kk'\cos\phi]^{1/2} , \tag{22}$$

$$\langle nm|V^{(1)}_{k,k'}|n'm'\rangle=\int dz\, f_n(z)f_{n'}(z) \times\int dz'\, g_m(z')g_{m'}(z) \times F(k,k',|z-z'|) , \tag{23}$$

$$F(k,k',|z-z'|)=\frac{e^2}{2\epsilon}\int_0^{\pi}d\phi\frac{1}{\pi q}(e^{-q|z-z'|}-1) , \tag{24}$$

and

$$V^{(2)}(q)=\frac{e^2}{2\epsilon q} . \tag{25}$$

Since $V^{(2)}(\mathbf{k}-\mathbf{k}')$ is still singular at $k=k'$, we subtract its singular part again

$$\sum_{\mathbf{k}'}\frac{1}{A}V^{(2)}(\mathbf{k}-\mathbf{k}')G_{nm}(\mathbf{k}',\Omega) =\int_0^{\infty}dk'\frac{k'}{2\pi}V^{(2)}_{k,k'}\left[G_{nm}(k',\Omega)-\frac{2k^2}{k^2+(k')^2}G_{nm}(k,\Omega)\right] + \sum_{\mathbf{k}'}\frac{e^2}{2\epsilon|\mathbf{k}-\mathbf{k}'|A}\frac{2k^2}{k^2+(k')^2}G_{nm}(k,\Omega) , \tag{26}$$

where

$$V^{(2)}_{k,k'}=\frac{e^2}{2\epsilon}\int_0^{2\pi}d\phi\frac{1}{2\pi}\frac{1}{[k^2+(k')^2-2kk'\cos\phi]^{1/2}} =\frac{e^2}{2\epsilon}\frac{1}{k+k'}\frac{2}{\pi}K(4kk'/(k+k')^2) \tag{27}$$

and K is the complete elliptic integral of the first kind:

$$K(x)=\int_0^{\pi/2}d\theta\frac{1}{\sqrt{1-x\sin^2\theta}} . \tag{28}$$

The second term on the right-hand side of Eq. (26) can be integrated analytically by a change of variables, $\mathbf{k}-\mathbf{k}'=\mathbf{k}''$, and integration over $\mathbf{k}''$:

$$\sum_{\mathbf{k}'}\frac{e^2}{2\epsilon|\mathbf{k}-\mathbf{k}'|A}\frac{2k^2}{k^2+(k')^2}=\frac{e^2k}{2\epsilon}\frac{C_0}{4\pi} , \tag{29}$$

where

$$C_0=\frac{4}{\sqrt{2}}\int_0^{\infty}dx\frac{1}{\sqrt{1+x^4}}=\frac{\Gamma(\frac{1}{4})\Gamma(\frac{1}{4})}{\sqrt{2}\Gamma(\frac{1}{2})}=5.244\,116 . \tag{30}$$

The factor $2k^2/[k^2+(k')^2]$ is chosen in (26) so that it equals 1 when $k=k'$, and it speeds up the convergence rate for large k'. Thus Eq. (19) becomes

$$[E_{nm}(k)-\Omega]G_{nm}(k,\Omega)-\sum_{n'm'}\int_0^{\infty}dk'\frac{k'}{2\pi}\langle nm|V^{(1)}_{k,k'}|n'm'\rangle G_{n'm'}(k',\Omega) -\int_0^{\infty}dk'\frac{k'}{2\pi}V^{(2)}_{k,k'}\left[G_{nm}(k',\Omega)-\frac{2k^2}{k^2+(k')^2}G_{nm}(k,\Omega)\right]-\frac{e^2k}{2\epsilon}C_0G_{nm}(k,\Omega)=\mu_{nm}(k) . \tag{31}$$

Using the exciton Bohr radius

$$a_B=\frac{4\pi\epsilon\hbar^2}{m_re^2} \tag{32a}$$

and

$$k_B=\frac{1}{a_B} , \tag{32b}$$

where m_r is the reduced effective mass, $1/m_r=1/m_e^*+1/m_h^*$, we normalize the lengths by the Bohr radius and the wave number k by k_B,

$$\underset{\sim}{k}=k/k_B . \tag{32c}$$

All the energies are normalized by the Rydberg for the exciton:

$$R_0=\frac{\hbar^2k_B^2}{2m_r}=\frac{m_re^4}{2(4\pi\epsilon)^2\hbar^2} . \tag{33}$$

We define

$$\underset{\sim}{G}_{nm}(\underset{\sim}{k},\underset{\sim}{\Omega})=\frac{R_0}{er_{cv}}G_{nm}(k,\Omega) , \tag{34a}$$

$$\underset{\sim}{\mu}_{nm}(\underset{\sim}{k})=\frac{1}{er_{cv}}\mu_{nm}(k) , \tag{34b}$$

$$r_{cv}\equiv\frac{\sqrt{2}\hbar M_b}{m_0E_G} . \tag{35}$$

The matrix elements μ_{nm}, r_{cv}, and M_b are given in Appendix A, and $\underset{\sim}{\Omega}=\Omega/R_0$. Equation (31) becomes

$$[\underset{\sim}{E}_{nm}(\underset{\sim}{k})-\underset{\sim}{\Omega}]\mathbf{G}_{nm}(\underset{\sim}{k},\underset{\sim}{\Omega})-\sum_{n'm'}\int_0^\infty d\underset{\sim}{k}'\frac{\underset{\sim}{k}'}{2\pi}\frac{k_B^2}{R_0}\langle nm|V^{(1)}_{\underset{\sim}{k},\underset{\sim}{k}'}|n'm'\rangle\underset{\sim}{G}_{n'm'}(\underset{\sim}{k}',\underset{\sim}{\Omega})$$
$$-\int_0^\infty d\underset{\sim}{k}'\frac{\underset{\sim}{k}'}{2\pi}\frac{k_B^2}{R_0}V^{(2)}_{\underset{\sim}{k},\underset{\sim}{k}'}\left[\underset{\sim}{G}_{nm}(\underset{\sim}{k}',\underset{\sim}{\Omega})-\frac{2\underset{\sim}{k}^2}{\underset{\sim}{k}^2+(\underset{\sim}{k}')^2}\underset{\sim}{G}_{nm}(\underset{\sim}{k},\underset{\sim}{\Omega})\right]-C_0\underset{\sim}{k}\mathbf{G}_{nm}(\underset{\sim}{k},\underset{\sim}{\Omega})=\underset{\sim}{\mu}_{nm}(\underset{\sim}{k}), \quad (36)$$

where $k_Be^2/(2\epsilon R_0)=4\pi$ has been used in the last term containing C_0. It also simplifies the terms containing $V^{(1)}$ and $V^{(2)}$ since both contain the same factors $k_B^2e^2/(2\epsilon R_0)$.

Let $\underset{\sim}{k}=\tan[(\pi/2)x]$ and use the Gaussian quadrature method for

$$\int_0^\infty d\underset{\sim}{k}\frac{\underset{\sim}{k}}{2\pi}F(\underset{\sim}{k})=\int_0^1 dx\frac{\underset{\sim}{k}}{4}(1+\underset{\sim}{k}^2)F(\underset{\sim}{k})$$
$$=\sum_i w_i\frac{\underset{\sim}{k}_i}{4}(1+\underset{\sim}{k}_i^2)F(\underset{\sim}{k}_i), \quad (37)$$

where w_i $(i=1,\ldots,N)$ are the weighting factors and $(\underset{\sim}{k}_i/4)(1+\underset{\sim}{k}_i^2)$ is the Jacobian. We define

$$W_i=w_i\frac{\underset{\sim}{k}_i}{4}(1+\underset{\sim}{k}_i^2), \quad (38)$$

$$\underset{\sim}{G}_{nm}(i)=\sqrt{W_i}\,\underset{\sim}{G}_{nm}(\underset{\sim}{k}_i,\underset{\sim}{\Omega}), \quad (39)$$

and

$$\underset{\sim}{\mu}_{nm}(i)=\sqrt{W_i}\,\underset{\sim}{\mu}_{nm}(\underset{\sim}{k}_i). \quad (40)$$

Then Eq. (36) can be written in terms of a matrix equation with a symmetric matrix A:

$$\sum_{n',m',j}(A^{nm,n'm'}_{i,j}-\underset{\sim}{\Omega}\delta_{nn'}\delta_{mm'}\delta_{ij})\underset{\sim}{G}_{n'm'}(j)=\underset{\sim}{\mu}_{nm}(i), \quad (41)$$

$$A^{nm,n'm'}_{i,j}=\left[\underset{\sim}{E}_{nm}(\underset{\sim}{k}_i)-C_0\underset{\sim}{k}_i+\sum_{l(\neq i)}\frac{k_B^2}{R_0}V^{(2)}_{\underset{\sim}{k}_i,\underset{\sim}{k}_l}W_l\frac{2\underset{\sim}{k}_i^2}{\underset{\sim}{k}_i^2+\underset{\sim}{k}_l^2}\right]\delta_{nn'}\delta_{mm'}\delta_{ij}-\sqrt{W_i}\left\langle nm\left|\frac{k_B^2}{R_0}V^{(1)}_{\underset{\sim}{k}_i,\underset{\sim}{k}_j}\right|n'm'\right\rangle\sqrt{W_j}$$
$$-\sqrt{W_i}\frac{k_B^2}{R_0}V^{(2)}_{\underset{\sim}{k}_i,\underset{\sim}{k}_j}\sqrt{W_j}(1-\delta_{ij})\delta_{nn'}\delta_{mm'}, \quad (42)$$

$$\epsilon_2=\mathrm{Im}\left[\frac{2}{V}\sum_{nm\mathbf{k}}\mu^*_{nm}(k)G_{nm}(k,\hbar\omega+i\Gamma)\right]=\mathrm{Im}\left[\frac{2e^2r_{cv}^2k_B^2}{LR_0}\sum_i\underset{\sim}{\mu}^*_{nm}(i)\underset{\sim}{G}_{nm}(i)\right]. \quad (43)$$

IV. ANALYTICAL RESULTS IN PURELY 2D AND QUAIS-2D LIMITS

A. Purely 2D limit

For a purely two-dimensional case, we write

$$\epsilon_2=\mathrm{Im}\left[\frac{2}{V}\sum_{\mathbf{k}}\mu^*(k)G(\mathbf{k},\hbar\omega+i\Gamma)\right], \quad (44)$$

where

$$G(\mathbf{k},\hbar\omega+i\Gamma)=\sum_X\frac{\phi^X(\mathbf{k})\sum_{\mathbf{k}'}\phi^{X*}(\mathbf{k}')\mu(\mathbf{k}')}{E_X-\hbar\omega-i\Gamma}. \quad (45)$$

If μ is independent of k (take $\mu=er_{cv}=$real), we recover the Elliott formula[27]

$$\epsilon_2=\frac{2\mu^2}{V}\sum_X\frac{\left|\sum_{\mathbf{k}}\phi^X(\mathbf{k})\right|^2\Gamma}{(E_X-\hbar\omega)^2+\Gamma^2}$$
$$=\frac{2\mu^2}{L}\sum_X|\Phi_X(\rho=0)|^2\frac{\Gamma}{(E_X-\hbar\omega)^2+\Gamma^2}, \quad (46)$$

where

$$\sum_{\mathbf{k}}\phi^X(\mathbf{k})=\sqrt{A}\,\Phi_X(\rho=0) \quad (47)$$

has been used. For the lowest bound state of the exciton, i.e., the $X=1s$ state,

$$\Phi_{1s}(\rho)=(2/\pi)^{1/2}\frac{2}{a_B}e^{-2\rho/a_B}. \quad (48)$$

Thus it is convenient to pull out the factor $1/a_B=k_B$, and normalize all the energies E_X, $\hbar\omega$, and Γ by the Rydberg

$$\epsilon_2=\frac{2\mu^2k_B^2}{LR_0}\sum_{X=\text{bound states}}|\underset{\sim}{\Phi}_X(\rho=0)|^2\frac{\underset{\sim}{\Gamma}}{(\underset{\sim}{E}_X-\hbar\underset{\sim}{\omega})^2+\underset{\sim}{\Gamma}^2}, \quad (49)$$

where $\underset{\sim}{\Phi}_X(\rho=0)=a_B\Phi_X(\rho=0)$, the dimensionless bound-state wave functions.

For continuum states[5]

$$\Phi_X(\rho=0)=\frac{1}{\sqrt{A}}\left[\frac{2}{1+e^{-2\pi/(ka_B)}}\right]^{1/2}, \quad (50)$$

where

$$ka_B=\sqrt{(E_X-E_G)/R_0}. \quad (51)$$

We thus have the Sommerfeld enhancement factor with

$$E=E_X-E_G=\hbar^2k^2/(2m_r)\ , \tag{52}$$

$$S(E)=\left|\sum_{\mathbf{k}}\phi^X(\mathbf{k})\right|^2=\frac{2}{1+e^{-2\pi/(ka_B)}}\ . \tag{53}$$

We can rewrite the summation over the continuum states in the form

$$\sum_X=A\int\frac{d^2\mathbf{k}}{(2\pi)^2}=A\frac{m_r}{2\pi\hbar^2}\int_0^\infty dE=A\frac{k_B^2}{4\pi R_0}\int_0^\infty dE\ . \tag{54}$$

Thus (46) becomes

$$\epsilon_2=\frac{\mu^2k_B^2}{2\pi R_0L}\int_0^\infty d\underset{\sim}{E}\frac{S(\underset{\sim}{E})\underset{\sim}{\Gamma}}{(\hbar\underset{\sim}{\omega}-\underset{\sim}{E}_G-\underset{\sim}{E})^2+\underset{\sim}{\Gamma}^2}\ , \tag{55}$$

where $\underset{\sim}{E}=E/R_0$.

Without the Coulomb enhancement factor [take $S(\underset{\sim}{E})=1$], the free-electron and free-hole absorption result is

$$\epsilon_2^{\text{free}}(\omega)=\frac{\mu^2k_B^2}{2\pi R_0L}\left[\frac{\pi}{2}+\tan^{-1}\left[\frac{\hbar\omega-E_G}{\Gamma}\right]\right]\ . \tag{56}$$

Using

$$\epsilon_{2\infty}\equiv\epsilon_2^{\text{free}}(\omega=\infty)=\frac{\mu^2k_B^2}{2R_0L} \tag{57}$$

we have the bound- and continuum-state contributions (49) and (55):

$$\frac{\epsilon_2}{\epsilon_{2\infty}}=4\sum_{X=\text{bound states}}|\Phi_X(\rho=0)|^2\frac{\underset{\sim}{\Gamma}}{(\underset{\sim}{E}_X-\hbar\underset{\sim}{\omega})^2+\underset{\sim}{\Gamma}^2}+\frac{1}{\pi}\int_0^\infty d\underset{\sim}{E}\frac{S(\underset{\sim}{E})\underset{\sim}{\Gamma}}{(\hbar\underset{\sim}{\omega}-\underset{\sim}{E}_G-\underset{\sim}{E})^2+\underset{\sim}{\Gamma}^2}\ . \tag{58}$$

B. Quasi-2D limit

1. The Green's-function method

For comparison purposes, we consider only one electron ($n=C1$) and one hole ($m=$HH1) state, and compare our numerical results using the exciton Green's function with those of the commonly used variational method. We can rewrite (43) as

$$\epsilon_2=\text{Im}\left[\frac{2}{V}\sum_{\mathbf{k}}\mu_{nm}^*(\mathbf{k})G_{nm}(\mathbf{k},\hbar\omega+i\Gamma)\right]=\frac{2\mu^2|I_{nm}^{eh}|^2}{VR_0}\sum_X\frac{\left|\sum_{\mathbf{k}}\phi^X(\mathbf{k})\right|^2\underset{\sim}{\Gamma}}{(\underset{\sim}{E}_X-\hbar\underset{\sim}{\omega})^2+\underset{\sim}{\Gamma}^2}\ . \tag{59}$$

We note that

$$\delta_{XX'}=\sum_{\mathbf{k}}\phi^{X*}(k)\phi^{X'}(k')=Ak_B^2\int_0^\infty d\underset{\sim}{k}\frac{\underset{\sim}{k}}{2\pi}\phi^{X*}(k)\phi^{X'}(k)=Ak_B^2\sum_i W_i\phi^{X*}(i)\phi^{X'}(i)\equiv\sum_i\underset{\sim}{\phi}^{X*}(i)\underset{\sim}{\phi}^{X'}(i)\ , \tag{60}$$

where $\underset{\sim}{\phi}^X(i)$ is the normalized eigenvector obtained directly from the computer solution (Appendix B). Thus, in terms of the normalized, dimensionless eigenvector $\underset{\sim}{\phi}^X(i)$, we have

$$\frac{\epsilon_2}{\epsilon_{2\infty}^f}=4\sum_X\frac{\left|\sum_i\underset{\sim}{\phi}^X(i)\right|^2\underset{\sim}{\Gamma}}{(\underset{\sim}{E}_X-\hbar\underset{\sim}{\omega})^2+\underset{\sim}{\Gamma}^2}\ , \tag{61}$$

where we have normalized ϵ_2 by the limiting free electron-hole result

$$\epsilon_{2\infty}^f=\frac{\mu^2k_B^2}{2R_0L}|I_{nm}^{eh}|^2\ . \tag{62}$$

The above expression (61) contains both the bound- and continuum-state contributions.

Let us compare the Green's-function method with the variational method.

2. Variational method (Ref. 1)

In this method, we assume the separable trial function for the 1s bound exciton

$$\Psi=f_n(z_e)g_m(z_h)\Phi(\rho)\ , \tag{63a}$$

$$\Phi(\rho)=(2/\pi)^{1/2}\frac{1}{\lambda}e^{-\rho/\lambda} \tag{63b}$$

and minimize the exciton energy

$$E_{\text{ex}}(\lambda)=\frac{\langle\Psi|H|\Psi\rangle}{\langle\Psi|\Psi\rangle}=E_n^e(0)+E_m^h(0)+\frac{\hbar^2}{2m_r\lambda^2}-\frac{e^2}{4\pi\epsilon}\frac{4}{\lambda^2}\int dz_e\,|f_n(z_e)|^2\int dz_h\,|g_m(z_h)|^2\int_0^\infty d\rho\,\rho\frac{e^{-2\rho/\lambda}}{[\rho^2+(z_e-z_h)^2]^{1/2}} \tag{64}$$

with respect to λ, where

$$H=\left[-\frac{\hbar^2}{2m_e^*}\frac{d^2}{dz_e^2}+V(z_e)+|e|Fz_e\right]+\left[-\frac{\hbar^2}{2m_h^*}\frac{d^2}{dz_h^2}+V(z_h)+|e|Fz_h\right]-\frac{\hbar^2}{2m_r}\nabla_\rho^2-\frac{e^2}{4\pi\epsilon[\rho^2+(z_e-z_h)^2]^{1/2}}\ . \tag{65}$$

It is convenient to write in terms of the normalized parameter

$$\tilde{\beta}=\frac{a_B}{\lambda}\ , \tag{66}$$

the normalized (dimensionless) wave function $\underset{\sim}{\Phi}(\rho)=a_B\Phi(\rho)$,

$$\underset{\sim}{\Phi}_{1s}(\rho)=(2/\pi)^{1/2}\tilde{\beta}e^{-\tilde{\beta}\rho/a_B}\ , \tag{67}$$

and the normalized binding energy $\underset{\sim}{E}_b = E_b/R_0$. The normalized binding energy $\underset{\sim}{E}_b$ is obtained from the last two terms in (64):

$$\langle \underset{\sim}{E}_b \rangle = \tilde{\beta}^2 - 4\tilde{\beta} \int dz_e \, |f_n(z_e)|^2 \times \int dz_h \, |g_m(z_h)|^2 G(2\tilde{\beta}|z_e - z_h|/a_B) , \tag{68}$$

where

$$G(x) = \int_0^\infty dt \frac{te^{-t}}{(t^2+x^2)^{1/2}} . \tag{69}$$

Here, unlike in Ref. 28, where the wave functions for $f_n(z_e)$ and $g_m(z_h)$ are obtained variationally, we find them numerically from a transition matrix method. We may also check the purely 2D limit by deleting the z dependence and using

$$G(0) = 1, \quad \langle \underset{\sim}{E}_b \rangle = \tilde{\beta}^2 - 4\tilde{\beta} . \tag{70}$$

Thus the minimum occurs at $\tilde{\beta} = 2$ and $\langle \underset{\sim}{E}_b \rangle_{\min} = -4$ as expected.

For a quantum-well problem, once $\tilde{\beta}$ is obtained, we find $\underset{\sim}{E}_b$ and $\underset{\sim}{E}_x = \underset{\sim}{E}_{nm} + \underset{\sim}{E}_b$, where

$$\underset{\sim}{E}_{nm} = [E_G + E_n^e(0) + E_m^h(0)]/R_0 ,$$

and the energy gap E_G has been added to Eq. (69) for the exciton energy E_X. The normalized imaginary part of the permittivity is

$$\frac{\epsilon_2}{\epsilon_{2\infty}^f} = \left[\frac{8\tilde{\beta}^2}{\pi} \right] \frac{\underset{\sim}{\Gamma}}{(\underset{\sim}{E}_X - \hbar\underset{\sim}{\omega})^2 + \underset{\sim}{\Gamma}^2} + \frac{1}{\pi} \int_0^\infty d\underset{\sim}{E} \frac{S(\underset{\sim}{E})\underset{\sim}{\Gamma}}{(\hbar\underset{\sim}{\omega} - \underset{\sim}{E}_{nm} - \underset{\sim}{E})^2 + \underset{\sim}{\Gamma}^2} . \tag{71}$$

V. NUMERICAL RESULTS AND DISCUSSIONS

In our numerical integrations, the Gaussian quadrature method has been used. Depending on the desired accuracy and the range of photon energy for calculation of the absorption coefficient, 48 quadrature points have typically been used for the absorption coefficients to be accurate with the photon energy larger than ten rydbergs above the band edge of the free electron-hole state. The actual calculations can be done either from solving for the Green's function using Eqs. (41)–(43) or solving for the exciton wave function directly using (10), (B1), and (B2) in Appendix B. Both methods give identical results. The computation time depends on how many optical energies $\hbar\omega$ are needed to plot the absorption spectrum. If we only need a few optical energies, it is more efficient to find the Green's function by directly inverting the matrix equation (41) and evaluating ϵ_2 using (43). If we require absorption spectrum at many optical energies, say, the number of $\hbar\omega$'s is much larger than the number of quadrature points for the k variable, it is computationally more efficient to solve for the exciton eigenvalues and eigenfunctions using (10) or (B1), and then evaluate ϵ_2 using Eq. (B2).

In Fig. 2, we compare the numerical results for the imaginary part of the normalized permittivity using the exciton Green's-function method, Eq. (61), with those using the variational method, Eq. (71). The horizontal axes are in terms of the normalized photon energy measured from the band-edge energy of the free electron-hole state in the exciton rydberg unit, $(\hbar\omega - E_G - E_n^e - E_m^h)/R_0$. We assume a GaAs/$Al_{0.3}Ga_{0.7}As$ quantum well of a width 100 Å without an applied electric field. The exciton half-linewidth is taken to be 1 rydberg (=3.88 meV). For comparison purposes, only one conduction subband and one heavy-hole subband are considered since the variational method usually uses the same assumption, which is a good approximation when the subband energy level difference is larger that the exciton binding energy. This is true in our case. The physical parameters used are $E_g = 1.425$ eV, $\epsilon = 12.15\epsilon_0$, $m_{hh}^*(x) = (0.34 + 0.42x)m_0$, $m_{lh}^*(x) = (0.094 + 0.043x)m_0$, and $m_e^*(x) = (0.0665 + 0.0835x)m_0$. In Fig. 2, the two dashed lines are calculated using the variational method for the bound exciton state: one with the 2D Sommerfeld enhancement factor, the other without the 2D enhancement factor for the continuum states. We find that the variational method gives an accurate binding energy ($E_b = -2.186R_0 = -8.5$ meV) compared with the value from the Green's-function method ($E_b = -2.226R_0 = -8.6$ meV). However, the oscillator strength differs from that of the Green's-function method by more than 20%. This is expected since in the variational method the energy, when minimized, has a second-order error when the trial wave function has a first-order error. Thus, the oscillator strength, which is proportional to the square of the wave function, is less accurate than the binding energy, percentage-wise. We also see that the 2D enhancement factor overestimates the absorption by about 50% in the continuum and produces a dip at the onset of the continuum, which is not observed experimentally. We have also compared the results of the Green's-

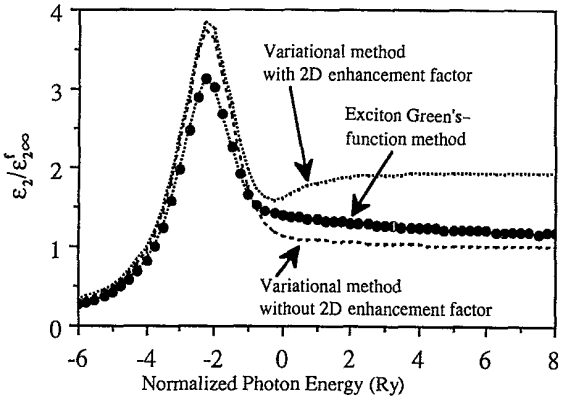

FIG. 2. The normalized imaginary part of the permittivity, $\epsilon_2/\epsilon_{2\infty}^f$, for a (100 Å GaAs)/$Al_{0.3}Ga_{0.7}As$ quantum well using the Green's-function method compared to the variational method with and without the Sommerfeld enhancement factor. The horizontal axis is in terms of $(\hbar\omega - E_G - E_1^e - E_1^h)/R_0$, the normalized photon energy measured from the subband edge.

function method with those using another variational method presented in Ref. 4. We found that the exciton binding energy differs more from the Green's-function method than that using the variational method shown here. This is because the Coulomb potential term is approximated using an average separation A instead of $(z_e - z_h)$ in the z dependence in the variational method of Ref. 4. Thus the Coulomb term becomes easier to evaluate in the minimization procedure of the variational approach, i.e., one integration for the vibrational method of Ref. 4 versus three integrations in Eqs. (68) and (69). The numerical result for the binding energy is -1.94 Ry, or -7.5 meV, and the oscillator strength for the bound state is underestimated by about 20%, while the continuum-state absorption is overestimated by more than 50%. This may also partially explain why the theoretical calculations of the absorption coefficients in Fig. 10 of Ref. 4 using the 2D-enhancement factor increase faster than for the experimental data as the photon energy is increased. The overestimations in the continua of all pairs of electron-hole subbands accumulate erros when a larger photon energy is considered.

In Figs. 3(a) and 3(b), we show the experimental results[2] of the $-\ln$(transmission) spectra of a 94-Å quantum-well structure with different applied electric fields for both the TE (the optical electric field is parallel to the plane of the layers) and TM polarizations (the optical field is perpendicular to the plane of the layers). Our numerical results using the Green's-function method are shown in Figs. 4(a) and 4(b) for the normalized absorption coefficients. We have used two heavy-hole and two electron subbands for the heavy-hole exciton and two light-hole and two electron subbands for the light-hole excitons. The exciton linewidths at different fields are taken from the experimental data. For the TE polarization in Fig. 4(a), both the heavy-hole and the light-hole excitons contribute to the absorption coefficient. With applied electric fields, the single-particle energies E_n^e and E_m^h are decreased for the lowest electron and hole subbands. The exciton binding energy is also slightly changed. The resultant red shifts of the peak ground-state exciton absorption are clearly seen with the reduction in the magnitude of the absorption coefficient mainly due to the reduction of the overlap integral. The peak absorption with a higher energy is due to the light-hole exciton. For the TM polarization, only the light-hole ex-

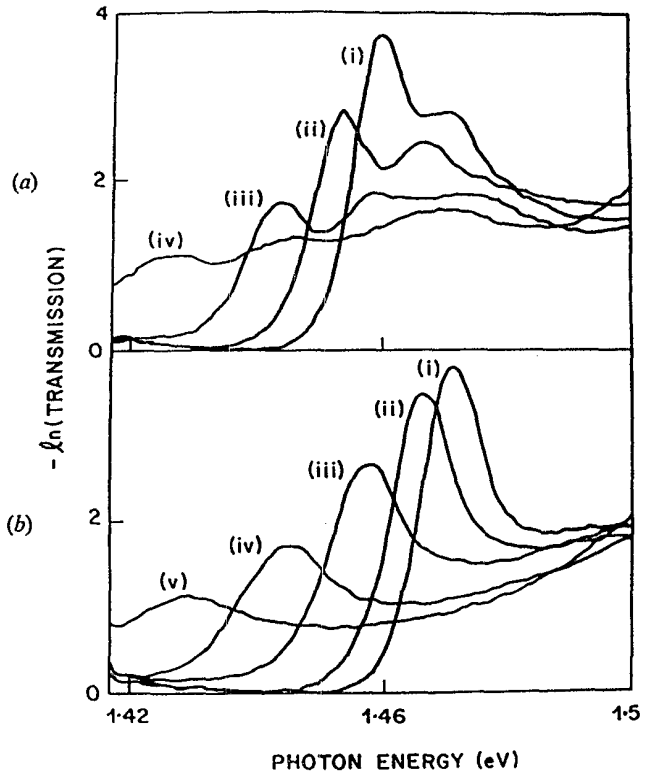

FIG. 3. Experimental $-\ln$(transmission) spectra of a (94 Å GaAs)/$Al_{0.3}Ga_{0.7}As$ quantum well. (a) The incident optical field is polarized parallel to the plane of the layers. The applied electric field is estimated to be (i) 0 V/cm, (ii) 6×10^4 V/cm, (iii) 1.0×10^5 V/cm, (iv) 1.5×10^5 V/cm. (b) The incident optical field is polarized perpendicular to the plane of the layers. The applied electric field is estimated to be (i) 0 V/cm, (ii) 6×10^4 V/cm, (iii) 1.1×10^5 V/cm, (iv) 1.5×10^5 V/cm. (From Refs. 2 and 3.)

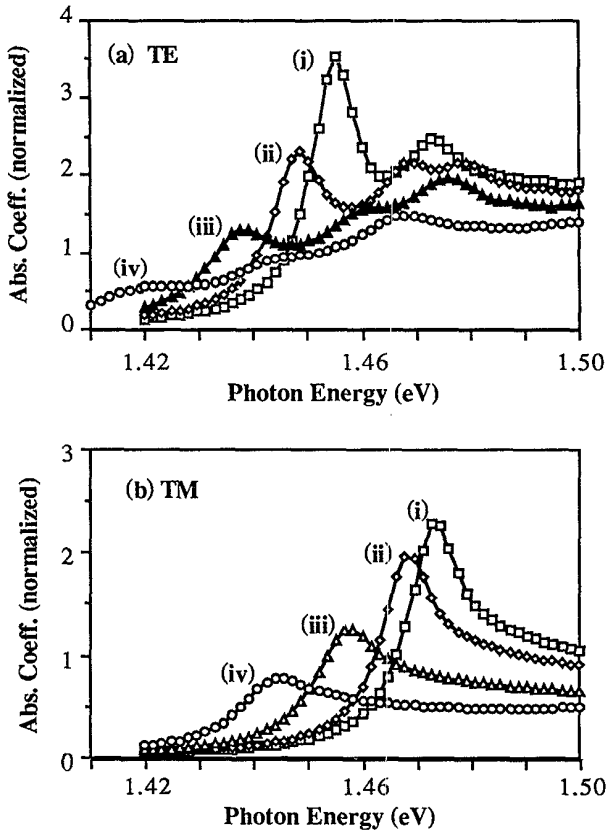

FIG. 4. Theoretical results using the Green's-function method for the normalized absorption coefficients of a (94 Å GaAs)/$Al_{0.3}Ga_{0.7}As$ quantum well. (a) The incident optical field is polarized parallel to the plane of the layers. The applied electric field is (i) 0 V/cm, (ii) 6×10^4 V/cm, (iii) 1.0×10^5 V/cm, (iv) 1.5×10^5 V/cm. (b) The incident optical field is polarized perpendicular to the plane of the layers. The applied electric field is (i) 0 V/cm, (ii) 6×10^4 V/cm, (iii) 1.1×10^5 V/cm, (iv) 1.5×10^5 V/cm.

citon contributes to the absorption. Even with the inclusion of the band mixing and the angular momentum effects (the azimuthal angle dependence), it has been shown[29,30] that the leading-order contribution of the heavy-hole exciton in the TM polarization is due to the $3d$ state and its magnitude is negligible compared to that of the light-hole $1s$ state. Thus the optical dipole moment for the HH1-$C1$ exciton state for TM polarization is taken to be zero. Generally speaking, our numerical results using the Green's-function method agree very well with the experimental results. There are still some discrepancies if an exact match of the theoretical and the experimental curves is desired. For example, the relative magnitudes of the heavy-hole and light-hole exciton absorptions and the broadening of the light-hole linewidth due to the coupling to the continuum of the heavy-hole exciton (the Fano resonance[10,11] effect) need further investigation. Further improvement of the theory is possible taking into account the valence-band mixing effects.

VI. CONCLUSIONS

An exciton Green's function is applied to study the optical absorption of quantum-well structures with applied electric fields. This method is quite general and is applicable to a quantum-well potential with an arbitrary profile. It also takes into account the bound and continuum exciton states in a consistent manner. In the conventional variational methods, the bound exciton wave function is obtained using a trial function and the continuum part is usually taken from the pure 2D-Sommerfeld enhancement factor. Thus, the bound states and the continuum states are not orthogonal to each other and do not form a complete set either. We compared our numerical results with those of the variational method and found that the variational method overestimates the absorption due to bound excitons by 20% and overestimates the absorption by more than 50% in the continuum when the pure 2D-enhancement factor is included. We have also compared our theoretical results with the experimental data, and found very good agreement. Further work on the inclusion of the valence-band mixing effects and/or applications to optical Stark effects is in progress.

ACKNOWLEDGMENTS

One of us (S.L.C.) thanks Y.-C. Chang and L. Tsang for interesting discussions. The work at the University of Illionois was supported by the U.S. Office of Naval Research (Grant No. N00014-90-J-1821). The computation time was supported through the National Center for Computational Electronics (NCCE) National Science Foundation Block Grant and we utilized the Cray Research, Inc. X-MP/48 computer at the National Center for Supercomputing Applications. Some of this work was performed while S.L.C. was visiting AT&T Bell Laboratories, Holmdel, New Jersey. He wishes to thank the technical staff for their hospitality.

APPENDIX A: POLARIZATION-DEPENDENT MATRIX ELEMENTS (REFS. 23–26, 29, AND 30)

The single-particle dipole moment can be related to the momentum matrix element $\mathbf{P}_{nm}(\mathbf{k})$,

$$\mu_{nm}(\mathbf{k})=e\mathbf{r}_{nm}(\mathbf{k}) =-\frac{i\hbar}{m_0}\frac{e\mathbf{P}_{nm}(\mathbf{k})}{E_{nm}(\mathbf{k})}, \tag{A1}$$

where m_0 is the electron mass in free space. The following approximate matrix elements are used based on the parabolic-band model.

TE polarization ($r=x$ or y):

$$\langle|\mu_{nm}(k)|^2\rangle=\left[\frac{e\hbar}{mE_{nm}(k)}\right]^2|I_{nm}^{eh}|^2 2M_b^2 \times\begin{cases}\frac{3}{4}(1+\cos^2\theta_{nm}), & \text{HH} \quad (A2a)\\ \frac{1}{4}(5-3\cos^2\theta_{nm}), & \text{LH}, \quad (A2b)\end{cases}$$

TM polarization ($r=z$):

$$\langle|\mu_{nm}(k)|^2\rangle=\left[\frac{e\hbar}{mE_{nm}(k)}\right]^2|I_{nm}^{eh}|^2 2M_b^2 \tag{A3a}$$

$$\times\begin{cases}0, & \text{HH}\\ \frac{1}{2}(1+3\cos^2\theta_{nm}), & \text{LH}, \quad (A3b)\end{cases}$$

where

$$I_{nm}^{eh}=\int f_n(z)g_m(z)dz, \tag{A4}$$

$$M_b^2=\frac{m_0^2E_G(E_G+\Delta)}{12m_e^*(E_G+\frac{2}{3}\Delta)}, \tag{A5}$$

$$\cos^2\theta_{nm}=\frac{E_{en}+E_{hm}}{E_{en}+E_{hm}+\hbar^2k^2/2m_r^*}. \tag{A6}$$

The heavy-hole contribution to the TM polarization case is taken as zero as discussed in the text and in Refs. 29 and 30. We define the dipole length

$$r_{cv}=\frac{\sqrt{2}\hbar M_b}{m_0E_G}. \tag{A7}$$

Then,

$$\mu_{nm}(k)=\frac{E_G}{E_{nm}(k)}I_{nm}^{eh}er_{cv}\sqrt{\tfrac{3}{4}(1+\cos^2\theta_{nm})} \tag{A8}$$

for the TE polarization, HH case.

For the bulk case, and if the k dependence of $\mu_{nm}(k)$ is ignored, we have

$$\mu\simeq er_{cv}. \tag{A9}$$

APPENDIX B: EIGENVALUES AND EIGENFUNCTIONS FOR THE EXCITON

An alternative way to find the reduced exciton Green's function is to solve the exciton eigenfunctions and eigenvalues directly from Eq. (10). The resultant matrix equations are similar to that of the Green's function

$$\sum_{n',m',j} A_{i,j}^{nm,n'm'} \underset{\sim}{\phi}^{X}_{n'm'}(j) = \underset{\approx}{E}_{X} \underset{\sim}{\phi}^{X}_{nm}(i) , \tag{B1}$$

where the normalized exciton wave function in the momentum space ϕ has been discussed in Eq. (60), and the matrix $A_{i,j}^{nm,n'm'}$ is the same as in Eq. (42). After obtaining the wave function $\underset{\sim}{\phi}$, the Green's function can be obtained from Eq. (13). In order to produce a continuous absorption spectrum, we may need to evaluate the absorption coefficient at many photon energies, $\hbar\omega$. When the number of photon energies is larger than the number of the quadrature points, it may be computationally faster to calculate the wave function $\phi(k)$ by solving for the eigenvector in (B1) and evaluating

$$\epsilon_0 \chi(\omega) = \frac{2}{V} \sum_{X} \frac{\left| \sum_{n,m,k} \phi_{nm}^{X}(\mathbf{k}) \mu_{nm}^{*}(\mathbf{k}) \right|^2}{E_X - \hbar\omega - i\Gamma} \tag{B2}$$

by summing over all the discretized exciton states X at each photon energy $\hbar\omega$.

[1] D. A. B. Miller, D. S. Chemla, T. C. Damen, A. C. Gossard, W. Wiegmann, T. H. Wood, and C. A. Burrus, Phys. Rev. B **32**, 1043 (1985).

[2] D. A. B. Miller, J. S. Weiner, and D. S. Chemla, IEEE J. Quantum Electron. **QE-22**, 1816 (1986).

[3] S. Schmitt-Rink, D. S. Chemla, and D. A. B. Miller, Adv. Phys. **38**, 89 (1989).

[4] J. Lee, M. O. Vassell, E. Koteles, and B. Elman, Phys. Rev. B **39**, 10 133 (1989). [Note there is a factory $\exp(\eta)$ missing in front of the exponential integral in Eq. (15).]

[5] M. Shinada and S. Sugano, J. Phys. Soc. Jpn. **21**, 1936 (1966).

[6] S. Hong and J. Singh, Superlatt. Microstruct. **3**, 645 (1987).

[7] G. D. Sanders and K. K. Bajaj, Phys. Rev. B **35**, 2308 (1987).

[8] G. D. Sanders and Y. C. Chang, Phys. Rev. B **35**, 1300 (1987).

[9] H. Chu and Y. C. Chang, Phys. Rev. B **39**, 10 861 (1989).

[10] D. A. Broido and L. J. Sham, Phys. Rev. B **34**, 3917 (1986).

[11] D. A. Broido, E. S. Koteles, C. Jagannath, and J. Y. Chi, Phys. Rev. B **37**, 2725 (1988).

[12] L. Hostler, Phys. Rev. **178**, 126 (1969).

[13] A. Stahl, Phys. Status Solidi B **94**, 221 (1979); A. Stahl and I. Balslev, *ibid.* **113**, 583 (1982).

[14] R. Zimmermann, Phys. Status Solidi B **135**, 681 (1986); **146**, 545 (1988).

[15] R. Zimmermann and M. Hartmann, Phys. Status Solidi B **150**, 365 (1988).

[16] S. Schmitt-Rink, D. S. Chemla, and H. Haug, Phys. Rev. B **37**, 941 (1988).

[17] S. Schmitt-Rink and D. S. Chemla, Phys. Rev. Lett. **57**, 2752 (1986).

[18] L. Tsang, D. Ahn, and S. L. Chuang, Appl. Phys. Lett. **52**, 697 (1988).

[19] L. Tsang, S. L. Chuang, and S. M. Lee, Phys. Rev. B **41**, 5942 (1990).

[20] Y. R. Shen, *The Principles of Nonlinear Optics* (Wiley, New York, 1984), Chap. 2.

[21] F. Bassani and G. Pastori Parravicini, *Electronic States and Optical Transitions in Solids* (Pergamon, New York, 1975), Chap. 6.

[22] L. Tsang and S.L. Chuang, Phys. Rev. B **42**, 5229 (1990).

[23] M. Yamanishi and I. Suemune, Jpn. J. Appl. Phys. **23**, L35 (1984).

[24] M. Yamanishi, S. Ogita, M. Yamagishi, K. Tabata, and N. Nakaya, Appl. Phys. Lett. **45**, 324 (1984).

[25] Y. Kan, H. Nagai, M. Yamanishi, and I. Suemune, IEEE J. Quantum Electron. **QE-23**, 2167 (1987).

[26] E. O. Kane, J. Phys. Chem. Solids **1**, 249 (1957).

[27] R. J. Elliott, Phys. Rev. **108**, 1384 (1957).

[28] S. Nojima, Phys. Rev. B **37**, 9087 (1988).

[29] B. Zhu and K. Huang, Phys. Rev. B **36**, 8102 (1987).

[30] B. Zhu, Phys. Rev. B **37**, 4689 (1988).

[31] Y. Kan, H. Nagai, M. Yamanishi, and I. Suemune, IEEE J. Quantum Electron. **QE-23**, 2167 (1987).